A Multi-MeV proton probe for Inertial Confinement Fusion/ Fast Ignitor studies

M Borghesi

Department of Pure and Applied Physics, The Queen's University, Belfast

D H Campbell, A Schiavi, O Willi*

The Blackett Laboratory, Imperial College of Science, Technology, and Medicine, London

A J Mackinnon

Lawrence Livermore National Laboratory, Livermore (CA, USA)

M Galimberti, L A Gizzi

IFAM-CNR, Pisa (Italy)

R J Clarke, S Hawkes

Central Laser Facility, CLRC Rutherford Appleton Laboratory, Chilton, Didcot, Oxon, OX11 0QX, UK

H Ruhl,

Max-Born-Insitut, Berlin (Germany)

Main contact email address: *m.borghesi@qub.ac.uk*

* present address: Institut für Laser-und-Plasmaphysik, Heinrich-Heine-Universität, Düsseldorf (Germany)

Introduction

In a number of experiments, performed with different laser systems and in different interaction conditions, protons with energies up to several tens of MeV have been detected behind thin foils irradiated with high intensity pulses[1,2]. In these experiments it was seen that the particle beams are directed along the normal to the back surface of the target, and have a small angular aperture at the highest energies. As proton beams are observed even using targets which nominally do not contain hydrogen, protons are thought to originate from hydro-carbon impurities located on the target surfaces or from bulk contamination of the target. Proposed theoretical models indicate that the protons gain their energy from the enormous electric field ($\sim$MeV/µm) set up by laser accelerated fast electrons via space-charge at the back target surface[3-5]. In particular, Particle-in-Cell simulations suggest that the proton beam charge will be globally neutralized by a co-moving cloud of MeV electrons [5]. The particular properties of these beams make them of great interest for application as a probe in high-density matter investigations. The use of protons as a radiographic source is an idea which has circulated for many years [6]. Applications of proton radiography have been proposed in the biomedical area or in testing of thick systems. Linear or cyclotron accelerators are used to obtain the proton energies required for these applications. Laser-produced proton beams represent a feasible alternative with enormous potential when high spatial/temporal resolution is required.

A particularly interesting application of laser-produced proton beams is the detection of electric and magnetic fields generated during the interaction of intense laser pulses with high density plasmas. In this context, proton imaging can be developed as a diagnostic with great potential for Inertial Confinement Fusion (ICF) studies. For example, the possibility of accessing directly electric field distributions in dense plasmas may shed new light on issues such as hydrodynamic and electromagnetic instabilities highly detrimental for ICF. The technique also has great potential for studying the complex and yet unexplored electric and magnetic field distributions in indirect drive target assemblies. In the Fast Ignitor context, it will contribute to the study of the large transient electric and magnetic fields generated in high-intensity laser-matter interactions. The magnitude and characteristics of these fields are currently the subject of much conjecture in the short pulse, high-intensity plasma physics community.

In this paper the principles of the technique and the results of a series of experimental tests, in which the proton source has been applied for the first time as a particle probe in a range of laser-plasma interaction conditions, will be presented and discussed.
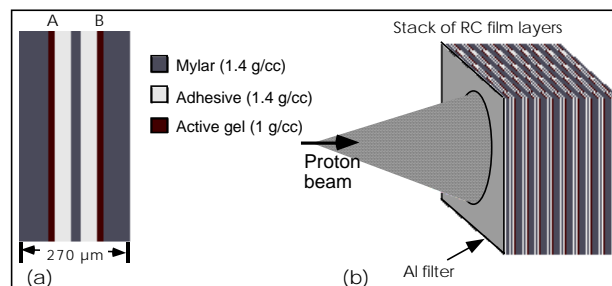

Figure1. Schematic of (a) a layer of Radiochromic film; (b) set-up for spectrally resolved proton beam detection.

Diagnostic set-up

The Vulcan Nd:glass laser operating in the Chirped Pulse Amplification mode (CPA) was used in the experiment. The main targets (used for the production of the proton beams) were Al foils, 1-2 mm wide and 3 - 25 µm thick. The 1.054 mm CPA interaction pulse, 1 ps in duration, with energy up to 100 J was focused by an F/3.5 off-axis parabola (OAP) onto the centre of the main target. The incidence was about 15° off normal. The focal spot varied between 8 and 10 µm in diameter at full width at half maximum (FWHM), containing 30-40 % of the energy, and giving intensities up to 5-7x10^{19} W/cm^2.

The detector employed in the experimental tests consisted of a stack of several layers of radiochromic (RC) film. As shown in Figure 1(a) the film consists of 270 µm thick plastic containing a double layer of organic dye, which reacts to ionizing radiation[7]. The equivalent dose of energetic protons stopped in the film can be measured from the changes in optical density undergone by the film, yielding information on the number and energy of the protons. By using them in a stack, each layer of film acts as a filter for the following layers. In fact protons deposit energy mainly in the Bragg peak at the end of their range[8]. Due to this, the contribution on each RC film layer will be mainly due to protons within a narrow energy range. The proton energies detectable as a function of the detector's depths are shown in Figure 2. Plastic track detectors were also used on some occasions to confirm that the structures observed were due to protons and not to electrons or x-rays to which the RC film is also sensitive. A 25 µm Al filter was placed in front of the first layer of film giving a minimum detectable proton energy of about 3 MeV.
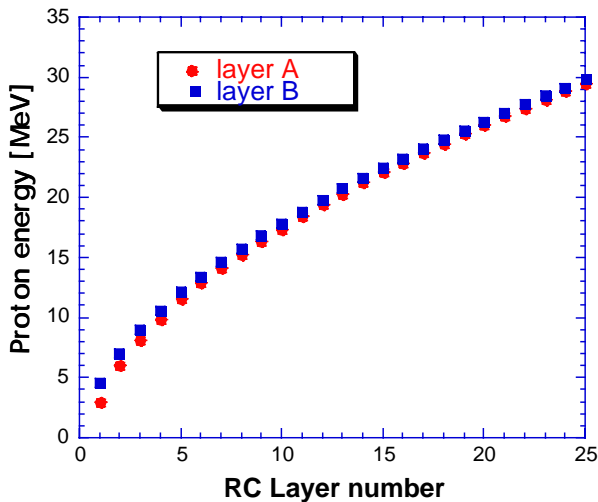
Figure 2. Proton energy detectable as a function of the RC film layer number.

Proton imaging

The laser-produced proton beam was characterized in view of its application as a particle beam probe. The protons were produced by focusing the CPA pulse onto the Al foil, and detected by placing the RC film stack at the back of the target, typically at a distance of about 2 cm. It was found that the proton beams have high brightness, typically with 10^{12} protons with energy above 3 MeV per shot and cutoff energy around 20 MeV (at a laser irradiance of the order of 5.10^{19} Wcm^{-2}). As observed in previous experiments, the beams were highly directional, propagating along the normal to the back surface of the target with small angular divergence (about 15° for 10 MeV protons). The energy deposited within each film layer can be extracted from the absolutely calibrated film. By doing this for each film layer and fitting an exponential energy spectrum, an estimate of the proton energy spectrum and total energy can be extracted from the film data[8]. The mean proton energy of the exponential fit is 3.75 MeV ± 0.3 MeV with a total energy of 2.2 J in an equivalent Maxwellian with a temperature of 2.5 MeV. During the experiments the source size of the proton beam was estimated using a penumbral edge method, setting an upper limit of 15-20 µm diameter for the source of 10 MeV protons.

The proton probe was used in a simple projection scheme, with the object placed between the proton source (i.e. the back side of the primary target) and the detector. With this arrangement some of the advantageous properties of the proton beam were successfully exploited, namely: the small source size, leading to high spatial resolution in imaging applications; the short pulse duration; the low divergence and high brightness of the beam. In addition, spatial and spectral resolution is guaranteed by an

appropriate choice of detector (e.g. RC film stacks), and the proton beam characteristics can be tuned by suitably changing the laser and target parameters. The temporal resolution obtainable with these beams is far beyond the possibilities of beams provided by conventional accelerators. Further, as it will be seen in the following sections, the fact that the beams have a broad spectrum is far from being a disadvantage when probing transient fields. Finally their ease of use and synchronization is a clear advantage in laser-plasma and Inertial Confinement Fusion related experiments; the fact that, being charged, protons can be used for diagnosing electric and magnetic fields, makes proton beam probing a powerful, novel diagnostic method, complementary to techniques such as x-ray radiography.

In general, the intensity distribution cross-section of a proton beam propagating through matter is modified both by collisional stopping/scattering, and by deflections due to electric and magnetic fields. In situations in which scattering/stopping are unimportant (e.g. thin targets) and there are no fields, there is a one-to-one correspondence between the object and detector planes (point projection imaging), as an effect of the small source size. The magnification of the image is simply determined by the ratio of the detector-to-object and object-to-source distances. Deflection due to electric or magnetic fields present in and around the object will introduce perturbations to this projection image. From such distortions, the electric and magnetic fields distribution at the object can be inferred. Depending on the target and irradiation geometry employed, the technique can be made more sensitive to the detection of electric rather than magnetic fields. 3D Particle-In-Cell simulations performed by Dr.H.Ruhl (MBI-Berlin) have studied the propagation of proton beams through plasmas. These simulations have confirmed that electric field structures present in the plasma (as for example those associated with small-scale density non-uniformities) can indeed be imprinted on the proton beam intensity profile. PIC/hydrodynamic simulations, coupled to post-processing via particle ray-tracing, will be fundamental for the retrieval of the field distribution in the more complex situations.

Imaging of cold solid objects

When thick solid obstacles were placed in the beam a shadow of the object was observed in the proton images, due to collisional stopping in the target. However, a shadow was observed even when objects with a thickness much smaller than the proton penetration depth were used, e.g. a mesh formed by 10 µm Cu wires with 25 or 100 µm spacing. The set-up for this particular test is depicted in Figure 3(a). The mesh was parallel to the main target, i.e. perpendicular to the proton beam. The distance between the proton source and the mesh was 1 mm, while the first of the radiochromic film layers was positioned at 22 mm from the source.
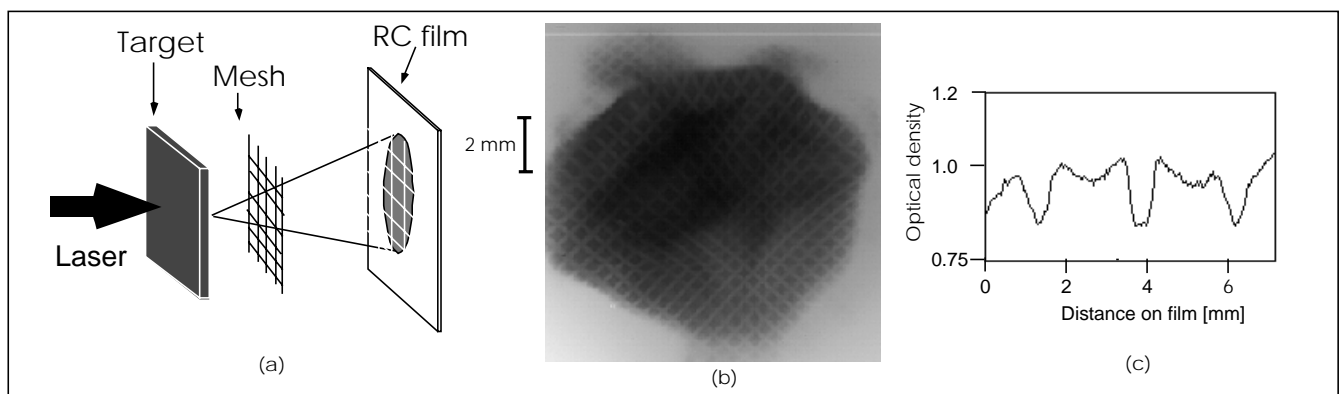

Figure 3. (a) Set up for proton imaging of a mesh; (b) image of a mesh with 25 µm spacing (10 µm Cu wires) obtained with 15 MeV protons; (c) Lineout across image of a mesh with 100 µm obtained with 20 MeV protons.

A shadow of the mesh was observed on the radiochromic film, as shown in Figure 3(b). The image shown in the picture has been obtained with 15 MeV protons and the 25 µm spacing mesh. The shadow of the wires can be observed clearly, the contrast of the picture being quite sharp. Figure 3(c) shows the optical density lineout across the shadow of a different mesh, with 100 µm spacing, obtained with 20 MeV protons. The magnification is consistent with the geometry of the imaging system. The optical density modulation observed is of the order of 0.2. It should be noted that the stopping range of 20 MeV protons in Cu is about 900 µm, and the collisional energy loss for such energetic protons in 10 µm of Cu is just $\Delta E/E \sim 5.10^{-3}$. Taking into account the film response, this would lead only to a variation in optical density $\Delta D \sim 5.10^{-5}$. Therefore the shadow observed must be due to some different effect. Our present explanation is that the mesh charges up positively, due, for example, to hot electrons preceding the proton beam and expelling a small number of cold electrons from the target via collisions. The deflection of the protons due to the electric field in the proximity of the wires is then responsible for the creation of the mesh shadow on the detector, where pile-up of the deflected protons is observed beside the regions of minimum transmission. An estimate of the linear charge on the mesh can be obtained via particle tracing, giving $\lambda \sim 10^{-6}$ C/m.

Imprinting of the electric field structures on the proton beam is indeed possible even if the beam is globally neutral, as predicted by PIC models. In fact, due to the low density of the proton beam when it reaches the object, and the high temperature of the electrons of the cloud, the Debye length of the ion-electron cloud will be several hundreds of microns (i.e. significantly larger than the spatial scale of the electric field structures).
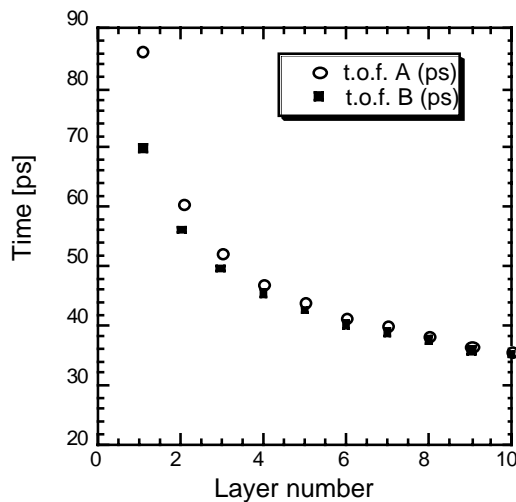

Figure 4. Time of arrival on target versus RC film layer number (data for both active layers A and B of each RC film is plotted).

Imaging of fast-evolving objects

When probing an object undergoing fast changes, the fact that the proton beams are not monochromatic is actually an advantage, as it can be exploited to obtain, in a single shot, information on the temporal history of the object to be probed. In fact, if the object to be probed is situated at a finite distance from the source, protons with different energies will reach the object at different times. By employing a detector that performs spectral selection, the information on the temporal evolution of the target can be retained. This is explained in Figure 4, where the calculated time of arrival on target of the protons produced on the Al foil is plotted versus the RC film layer number (i.e. versus their energy). As can be seen, the presence of the double active layer in each RC film causes a temporal indetermination

which is larger for the first RC layers, but can be removed by mechanically separating the two gel layers after data collection.

By doing so, we were able to confirm the short duration of the proton burst. Figure 5 shows a scan of the two parts of an RC film layer after separation. The object being probed was a solid target (50 µm Ta wire) irradiated with a second CPA pulse. More details about the experimental arrangement for this experiment are given elsewhere in this Annual Report [10]. The target charges up following the interaction, and the proton beam probes a fast evolving electric field pattern. The RC film layer of Figure 5 was the second in the film stack, and the signal of the A and B active layers is mainly due, respectively, to 6 and 7 MeV protons. The temporal difference on target between protons with this energy is about 5 ps. As is clearly visible, the patterns observed in the two layers differ significantly, meaning that the protons producing the pattern have experienced different electric field configuration. From this it can be inferred that the duration of the proton burst at the source is smaller than 5 ps.
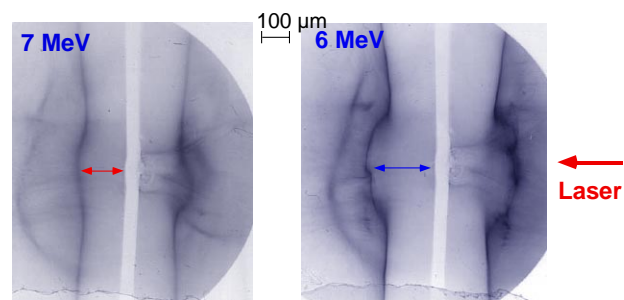

Figure 5. Proton images of a 50 µm Ta wire irradiated by a 10^{19} W/cm^2 pulse, obtained in the same event with 6 and 7 MeV protons. The spatial scale refers to the target plane.

Conclusion

Proton imaging is a diagnostic with great potential in laser-plasma interaction studies, which can allow diagnostic access to previously inaccessible phenomena. Some applications of the technique are detailed elsewhere in this report [10]. The work was supported by an ESPRC grant. We acknowledge the invaluable contribution to the work provided by the CLF staff.

References

1. E. L. Clark *et al,* Phys. Rev. Lett, 84 670 (2000)

2. R D Snavely *et al,* Phys. Rev. Lett., 85, 2945 (2000)

3. S.Wilks *et al,* Phys. Plasmas, 8, 542 (2001)

4. A.Pukhov *et al,* Phys. Rev. Lett, 86, 3562 (2001)

5. H.Ruhl *et al,* Plasma Phys. Rep., 27, 363 (2001)

6. A M Koehler, Science, 160, 303 (1968)

7. W.L.C.McLaughlin et al, Nucl. Instr. Methods Phys. Res. A 302, 165 (1991)

8. J. F. Ziegler, J. P.Biersack and U. Littmark, The Stopping and Range of Ions in Solids, Pergamon Press, New York, 1985

9. A J MacKinnon *et al,* Phys. Rev. Lett., 86, 1769 (2001)

10. M Borghesi *et al,* A Schiavi *et al,* in this volume